Large magnonic band gaps and defect modes in one-dimensional comblike structures

H. Al-Wahsh,* A. Akjouj,† B. Djafari-Rouhani, J. O. Vasseur, and L. Dobrzynski
Equipe de Dynamique des Interfaces, Laboratoire de Dynamique et Structures des Matériaux Moléculaires, U.P.R.E.S.A. C.N.R.S. No. 8024, U.F.R. de Physique, Université de Lille I, 59655 Villeneuve d'Ascq Cédex, France

P. A. Deymier
Department of Materials Science and Engineering, University of Arizona, Tucson, Arizona 85721
(Received 27 July 1998; revised manuscript received 5 October 1998)

We report the existence of large gaps in the band structure of a comblike structure composed of a one-dimensional magnonic waveguide along which N' dangling side branches are grafted at N equidistant sites. These gaps originate not only from the periodicity of the system but also from the resonance states of the grafted branches (which play the role of resonators). The width of these gaps is sensitive to the length of the side branches as well as to the numbers N and N'. The presence of defect branches in the comblike structure can give rise to localized states inside the gaps. We show that these states are very sensitive to the length of the side branches, to the periodicity, to N or/and N' and to the length of the defect branches. Analytic expressions are given for the band structure of combs for large N and for the transmission coefficient for an arbitrary value of N and N' with and without defects. [S0163-1829(99)09313-3]

I. INTRODUCTION

Low-dimensional magnets, materials in which magnetism arises from a configuration with a dimensionality less than three, have been shown both theoretically and experimentally to exhibit fascinating collective behaviors.[1–3] During the last decade several studies have addressed the problem of magnon band structures in one-dimensional magnetic composites such as superlattices. Most of these studies focus attention on the existence of stop bands in the spin-wave spectra of magnetic superlattices. Albuquerque *et al.*[4] calculated the dispersion relation for spin waves propagating in a general direction of an infinite superlattice made of two alternating ferromagnetic layers. They showed that in a certain frequency domain the superlattice dispersion curves exhibit broad pass bands and narrow stop bands. Dobrzynski, Djafari-Rouhani, and Puszkarski[5] investigated the existence of surface-localized magnons in the spin-wave spectra of semi-infinite ferromagnetic superlattices. Barnas[6] analyzed theoretically the spin-wave spectra of infinite, semi-infinite, and finite ferromagnetic superlattices in the exchange-dominated region. Hinchey and Mills[7] have carried out the study of magnetic properties of superlattices constructed by alternating films of ferromagnetic and antiferromagnetic layers. More recently, Vasseur *et al.*[8] calculated the spin-wave spectra of two-dimensional composite materials consisting of periodic square arrays of parallel cylinders made of a ferromagnetic material embedded in a ferromagnetic background. They also demonstrate that the existence of the stop bands was related to the physical parameters of the materials involved. Owing to the analogy between magnonic excitations and other excitations, the subject of propagation of elastic waves,[9] acoustic waves,[10] and electronic waves[11] in composite and low-dimensional media has received wide attention. It is worth mentioning that the interest in the systems exhibiting complete or pseudogaps was initiated by the pioneering experimental work of Yablonovitch on macroscopic photonic crystals in 1987.[12]

A search for composite systems that exhibit complete stop bands in their excitation spectra is motivated both by practical and fundamental reasons. From the practical point of view, such systems can be used to design filters that prohibit the corresponding waves at certain frequencies while allowing free propagation at others. From the fundamental point of view, John's proposal pointing out that the existence of complete photonic band gaps could lead to the Anderson localization of light in disordered photonic crystals[13] suggests that wave propagation in slightly perturbed periodic composites can lead to novel phenomena. It is worth mentioning that the original concept of classical wave localization was put forward in a classic paper by John in 1984.[14] A systematic account of the theoretical and experimental work on band-gap crystals and Anderson localization is compiled in a recent extensive review article.[15] Also, the problem of the emergence of localized states in the photonic band gaps by introducing defects in the periodic structure, for instance by removing or adding some inclusions[16–19] or by changing the characteristics (material or diameter) of several inclusions, has been addressed recently.[20] These properties have also started to be investigated in quasi-one-dimensional photonic crystals.[16,21]

Research in the area of high-temperature superconductors has spurred renewed interest into the properties of low-dimensional magnetic systems constituted of networks of quasi-one-dimensional chains. For instance, one of the most exciting recent developments in this direction has been the discovery of superconductivity in the doped $S=1/2$ ladder system $Sr_{0.4}Ca_{13.6}Cu_{24}O_{41.84}$ under pressure.[22] In these materials ladders, located in two-dimensional crystal layers, are composed of parallel one-dimensional chains of copper and

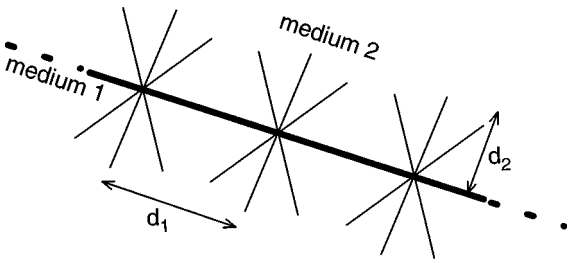

FIG. 1. Schematic of the one-dimensional waveguide studied in the present work. The material media are designated by an index i, with i equal 1 for the backbone (heavy line) and 2 for the dangling side branches (DSB). There are $N'(=6)$ DSB of length d_2 grafted at equidistant sites separated by a length d_1.

oxygen atoms linked by ''rungs'' of additional oxygen atoms. On the other hand recent improvements in manufacturing techniques that permit the fabrication of extremely thin wires of transition metals[23–25] (especially grown by decoration of atomic steps) offer hope for the fabrication of continuous quasi-one-dimensional wires of magnetic materials. Furthermore, advancements in the modern semiconductor technology that allow for the fabrication of nanostructures with controllable chemical composition and geometry such as quantum wires, dots, rings, crossbars, etc,[26] suggest the possibility in a near future of designing and manufacturing networks of one-dimensional magnetic wires. One can notice that these improvements have been used to design quasi-one-dimensional photonic band-gap waveguide at the submicrometer scale.[16,21] These recent developments have encouraged us to undertake a theoretical investigation of magnetic excitations in networks composed of one-dimensional continuous magnetic media. The present study focuses on a simple one-dimensional comblike structure with multiple dangling side branches (MDSB) (see Fig. 1). The geometry of the side branch attached to a waveguide has the peculiar property of giving rise to zeros of transmission along the waveguide.[27,28] These zeros of transmission occur at particular frequencies that are related to the length and physical characteristics of the side branch. These frequencies broaden into gaps when several side branches are grafted at equidistant nodes along the waveguide. This work demonstrates that the widths of the pass bands (and hence of the stop bands) in the magnonic band structure can be controlled by appropriate modification of the geometry and the chemical nature of the network's constituents. The properties of the magnetic networks are calculated within the framework of the interface response theory (IRT) of continuous media.[29] In addition to the excitation spectra of periodic comb structures, we have also calculated the transmission spectra of finite combs. Finally, we address the issue of the existence of localized states in the forbidden bands of the magnonic band structure. Such localized states result from the presence of a defect side branch inside the comb. Let us mention that semiconductor *T*-shaped structure,[28,30] serial stub structures,[31] as well as one-dimensional wires with DSB[32] have also been emphasized to have useful applications in electronic devices or interesting fundamental properties.

The outline of this paper is as follows. In Sec. II we initially review the IRT of continuous media. This theory allows the calculation of the Green's functions (GF) of a network structure in terms of the GF of its elementary constituents. In the second part of Sec. II, we use the IRT and the semiclassical torque equation for the magnetization to determine the magnetic GF for an infinite Heisenberg ferromagnetic medium. This GF provides a basis for the description of the bulk spin waves. We then give the inverse of the surface Green's function for a semi-infinite medium with a free end as well as the GF for a finite wire of length d. In Sec. III, we calculate the dispersion relation of a waveguide composed of N' DSB grafted periodically along an infinite wire. In addition to the band structure of the infinite periodic waveguide, we derive an expression for the transmission coefficient of a finite comb. This finite comb is constituted from the same N' DSB arranged on N equidistant sites along an infinite wire. Section IV is devoted to the analysis of the effect of geometry and materials on the band gap and the transmission coefficient of the networks. The appearance of localized modes inside the gaps when a defect side branch is inserted in the waveguide is examined in Sec. V. Finally, some conclusions are drawn in Sec. VI.

II. THEORETICAL MODEL

A. Interface response theory of continuous media: Overview

In this paper, we study the propagation of spin waves in composite systems composed of one-dimensional segments (or side branches) grafted on a one-dimensional substrate waveguide (or backbone). This study is performed with the help of the IRT (Ref. 29) of continuous media that permits the calculation of the Green's function of any composite material in terms of the GF of its elementary constituents. In the following, we present a brief review of the basic concepts and the fundamental equations of this theory.

Let us consider any composite material contained in its space of definition D and formed out of N different homogeneous pieces situated in their domains D_i. Each piece is bounded by an interface M_i, adjacent in general to j $(1 \leqslant j \leqslant J)$ other pieces through subinterface domains M_{ij}. The ensemble of all these interface spaces M_i will be called the interface space M of the composite material.

The elements of the Green's function $\mathbf{g}(DD)$ of any composite material can be obtained from[29]

$$\mathbf{g}(DD)=\mathbf{G}(DD)-\mathbf{G}(DM)\mathbf{G}^{-1}(MM)\mathbf{G}(MD) + \mathbf{G}(DM)\mathbf{G}^{-1}(MM)\mathbf{g}(MM)\mathbf{G}^{-1}(MM)\mathbf{G}(MD), \tag{1}$$

where $\mathbf{G}(DD)$ is the Green's function of a reference continuous medium and $\mathbf{g}(MM)$, the interface elements of the Green's function of the composite system. The inverse $\mathbf{g}^{-1}(MM)$ of $\mathbf{g}(MM)$ are obtained for any point in the space of the interfaces $M=\{\cup M_i\}$ as a superposition of the different $\mathbf{g}_i^{-1}(M_i,M_i)$,[29] the inverses of $\mathbf{g}_i(M_i,M_i)$ for each constituent i of the composite system. The latter quantities are given by the equation

$$\mathbf{g_i}^{-1}(M_i,M_i)=\mathbf{\Delta_i}(M_i,M_i)\mathbf{G_i}^{-1}(M_i,M_i), \tag{2}$$

where

$$\Delta_{\mathbf{i}}(M_i,M_i)=\mathbf{I}(M_i,M_i)+\mathbf{A}_{\mathbf{i}}(M_i,M_i),\quad(\mathbf{I}\text{ is the unit matrix}) \tag{3}$$

and

$$\mathbf{A}_{\mathbf{i}}(\mathbf{X},\mathbf{X}')=\mathbf{V}_{c_i}(\mathbf{X}'')\mathbf{G}_{\mathbf{i}}(\mathbf{X}'',\mathbf{X}')|_{\mathbf{X}''=\mathbf{X}}, \tag{4}$$

where $\{\mathbf{X},\mathbf{X}''\}\in M_i$ and $\mathbf{X}'\in D_i$.

In Eq. (4), the cleavage operator $\mathbf{V}_{c_i}$ acts only in the surface domain M_i of D_i and cuts a finite or semi-infinite size block out of the infinite homogeneous medium.[29] $\mathbf{A}_i$ is called the surface response operator of block *i*.

The new interface states can be calculated from[29]

$$\det[\mathbf{g}^{-1}(MM)]=0 \tag{5}$$

showing that, if one is interested in calculating the interface states of a composite, one only needs to know the inverse of the Green's function of each individual block in the space of their respective surfaces and/or interfaces.

Moreover if $\mathbf{U}(D)$ (Ref. 33) represents an eigenvector of the reference system, Eq. (1) enables the calculation of the eigenvectors $\mathbf{u}(D)$ of the composite material

$$\mathbf{u}(D)=\mathbf{U}(D)-\mathbf{U}(M)\mathbf{G}^{-1}(MM)\mathbf{G}(MD)+\mathbf{U}(M)\mathbf{G}^{-1}(MM)\mathbf{g}(MM)\mathbf{G}^{-1}(MM)\mathbf{G}(MD). \tag{6}$$

In Eq. (6), $\mathbf{U}(D)$, $\mathbf{U}(M)$, and $\mathbf{u}(D)$ are row vectors. Equation (6) provides a description of all the waves reflected and transmitted by the interfaces, as well as the reflection and the transmission coefficients of the composite system. In this case, $\mathbf{U}(D)$ must be replaced by a bulk wave launched in one homogeneous piece of the composite material.[33]

B. Inverse surface Green's functions of the elementary constituents

We report here the expression for the Green's function of a homogeneous infinite ferromagnetic medium. We give also the inverse of the surface Green's function for a semi-infinite medium with a free surface and for a slab of thickness *d* (or segment of length *d*).

1. Green's function for an infinite ferromagnetic medium

Here we turn to the calculation of the magnetic GF's for an infinite ferromagnetic medium. In using the Heisenberg model of a ferromagnet we are neglecting the effects of dipole-dipole interactions compared with the exchange contribution to the Hamiltonian. Therefore, in evaluating the needed Green's function, it is convenient to use a continuum approximation. Such an approximation is valid provided that the relevant wavelengths are large compared with the lattice spacing. Therefore, we will deal only with long-wavelength excitations.

A medium denoted ''*i*'' and described in a Cartesian coordinate system (O,x_1,x_2,x_3) is assumed to have a simple cubic structure with lattice parameter *a*. We take the spontaneous magnetization M_0 to be in the x_1 direction. The equation of motion for the total magnetization $\mathbf{M}$ can be expressed in terms of the total effective magnetic field $\mathbf{H}$ as

$$\frac{d\mathbf{M}}{dt}=\gamma(\mathbf{M}\times\mathbf{H})-\Gamma(\mathbf{M}-M_0 i_1), \tag{7}$$

where γ is the gyromagnetic ratio and Γ is a phenomenological damping factor (considered to be a positive constant). The fields $\mathbf{M}$ and $\mathbf{H}$ are given by

$$\mathbf{M}=M_0 i_1+\mathbf{m}(\mathbf{r},t), \tag{8a}$$

$$\mathbf{H}=H_0 i_1+\mathbf{h}_{\rm ex}(\mathbf{r},t)+\mathbf{H}_{\rm ext}\exp[j(\mathbf{k}.\mathbf{r}-\omega t)]. \tag{8b}$$

It is understood that i_1 is a unit vector parallel to the static fields M_0 and H_0 in the x_1 direction and $\mathbf{m}(\mathbf{r},t)$ represents the instantaneous deviation from its average value $M_0 i_1$. The term proportional to $\mathbf{H}_{\rm ext}$ in Eq. (8b) represents an externally applied driving field of wave vector $\mathbf{k}$ and frequency ω. Finally the term $\mathbf{h}_{\rm ext}(\mathbf{r},t)$ in (8b) is an effective field arising from the exchange interactions between neighboring magnetic moments. This exchange field $\mathbf{h}_{\rm ex}(\mathbf{r},t)$ may be written as,[34]

$$\mathbf{h}_{\rm ex}(\mathbf{r},t)=\frac{2}{(\gamma\hbar)^2}\sum_{\delta}J_{r,r+\delta}\mathbf{M}(\mathbf{r}+\boldsymbol{\delta},t), \tag{9}$$

where $J_{r,r+\delta}$ is the exchange interaction between magnetic sites at $\mathbf{r}$ and $\mathbf{r}+\boldsymbol{\delta}$. In this paper, we assume that $J_{r,r+\delta}$ couples only nearest neighbors in the simple cubic lattice. On expanding $\mathbf{M}(\mathbf{r}+\boldsymbol{\delta},t)$ in terms of $\mathbf{M}(\mathbf{r},t)$ and its derivatives using Taylor series, taking into account that for each site $\mathbf{r}$ there are six neighbors coupled by the exchange *J*, we obtain to the lowest order that,

$$\mathbf{h}_{\rm ex}(\mathbf{r},t)=\frac{2J}{(\gamma\hbar)^2}[6+a^2\nabla^2]\mathbf{M}(\mathbf{r},t). \tag{10}$$

Note that in doing the above expansion we use a continuum representation of the ferromagnet, as was mentioned before, and thus we are restricting ourselves to long-wavelength excitations. Inserting Eqs. (8a), (8b), and (10) into the torque Eq. (7), and making the usual linear spin-wave approximation (i.e., neglecting small terms that are of the second order in $\mathbf{m}$, since $|\mathbf{m}|\ll M_0$ at low temperatures) we arrive at the following equation of motion for $\mathbf{m}$,

$$\frac{d\mathbf{m}}{dt}+\Gamma\mathbf{m}=i_1\times\{\gamma M_0\mathbf{H}_{\rm ext}\exp[j(\mathbf{k}.\mathbf{r}-\omega t)]-(\gamma H_0-D'\nabla^2)\mathbf{m}\}, \tag{11}$$

where $D'=(2Ja^2M_0/\gamma\hbar^2)$. From the property of translational invariance of the medium and on assuming a time dependence in the form $\exp(-j\omega t)$, we may write

$$\mathbf{m}(\mathbf{r},t)=\mathbf{m}(x_3)\exp[j(\mathbf{k}_{\|}\cdot\mathbf{l}-\omega t)], \tag{12}$$

where $\mathbf{k}_{\|}\equiv(k_1,k_2)$ and $\mathbf{l}\equiv(x_1,x_2)$ are two-dimensional wave vectors. If we now substitute Eq. (12) into (11), after

some algebraic manipulations we arrive at the following differential equation for $m^+(x_3)$,

$$\frac{D'}{\gamma M_0}\left(\frac{\partial^2}{\partial x_3^2}-\mathbf{k}_\parallel^2+\frac{\omega+j\Gamma-\gamma H_0}{D'}\right)\mathbf{m}^+(x_3) = -(H_{\text{ext}}^{x_3}+jH_{\text{ext}}^{x_2})\exp(jk_3x_3), \tag{13}$$

where $m^+(x_3)=m_3(x_3)+jm_2(x_3)$, and $m_1(x_3)=0$. k_3 is the x_3 component of the propagation vector $\mathbf{k}=(\mathbf{k}_\parallel,\mathbf{k}_3)$. Now we are in a position to calculate the Green's function we need. On using Eq. (13) the Fourier-transformed Green's function between two points (sites) $\mathbf{r}(x_1,x_2,x_3)$ and $\mathbf{r}'(x_1',x_2',x_3')$ of the considered infinite ferromagnetic medium ''i'' associated with the magnetization $m^+(x_3)$ satisfies the following equation

$$\frac{F_i}{\alpha_i}\left(\frac{\partial^2}{\partial x_3^2}-\alpha_i^2\right)G_i(\mathbf{k}_\parallel,x_3,x_3')=\delta(x_3-x_3') \tag{14}$$

and can be expressed as[35]

$$G_i(\mathbf{k}_\parallel,x_3,x_3')=-\frac{e^{-\alpha_i|x_3-x_3'|}}{2F_i}, \tag{15}$$

where

$$\alpha_i=\left[\mathbf{k}_\parallel^2-\frac{\omega-\gamma_iH_0}{D_i'}\right]^{1/2} \tag{16a}$$

and

$$F_i=\frac{D_i'\alpha_i}{\gamma_iM_{0i}}. \tag{16b}$$

Let us note that Eq. (15) may be generalized to other excitations, such as elastic waves in solids or liquids,[33] electrons,[36] and electromagnetic waves.[37] In Eq. (16a) and in what follows, the damping constant Γ is considered to be zero. The Green's function for a one-dimensional infinite waveguide is obtained by setting $\mathbf{k}_\parallel=0$ in Eq. (16), i.e., $\alpha_i=j\sqrt{(\omega-\gamma_iH_0)/D_i'}=j\alpha_i'$.

2. Inverse surface Green's functions of the semi-infinite medium

One considers a semi-infinite medium ''i'' with a ''free surface'' located at the position $x_3=0$ in the direction Ox_3 of the Cartesian coordinate system (O,x_1,x_2,x_3) and infinite in the other two directions. In this case

$$g_i^{-1}(MM)=g_i^{-1}(00)=-F_i. \tag{17}$$

3. Inverse surface Green's functions of a slab (or segment)

One considers a slab of width d_i bounded by two free surfaces located at $x_3=0$ and $x_3=d_i$ in the direction Ox_3 of the Cartesian coordinates system (O,x_1,x_2,x_3) and infinite in the two other directions. In this case

$$g_i^{-1}(MM)=\begin{pmatrix}-\frac{F_iC_i}{S_i} & \frac{F_i}{S_i}\\ \frac{F_i}{S_i} & -\frac{F_iC_i}{S_i}\end{pmatrix} =\begin{bmatrix}g_i^{-1}(0,0) & g_i^{-1}(0,d_i)\\ g_i^{-1}(d_i,0) & g_i^{-1}(d_i,d_i)\end{bmatrix}, \tag{18}$$

where F_i has the same meaning as above and

$$C_i=ch(\alpha_id_i), \tag{19a}$$

$$S_i=sh(\alpha_id_i). \tag{19b}$$

One can see that in the interface domain M corresponding to the interfaces $x_3=0$ and $x_3=d_i$, the surface Green's function is a 2×2 square matrix. To obtain the Green's function for one-dimensional segments of waveguides, one needs only to take the limit $\mathbf{k}_\parallel\to0$ in Eq. (18). In order to study elementary spin-wave excitations, we calculate the Green's function in the interface space for a one-dimensional infinite backbone with a periodic array of MDSB.

III. BAND STRUCTURES AND TRANSMISSION COEFFICIENTS

A. One-dimensional infinite backbone with periodic array of MDSB

Here, we treat the case of a comblike structure composed of an infinite one-dimensional waveguide or backbone (medium 1), along which N' finite side branches (medium 2) of length d_2 are grafted periodically with spacing period d_1 at N sites, N and N' being integers (see Fig. 1). Let us first write the Green's function of this composite system. The infinite line can be modeled as an infinite number of finite segments (i.e., one-dimensional slab) of length d_1 in the direction x_3, each one being pasted to two neighbors. The interface domain is constituted of all the connection points between finite segments. Each connection point (site) on the infinite chain will be defined by the integer n such that $-\infty<n<+\infty$. On each site n, N' DSB of length d_2 are connected. Here and afterwards the cross sections of all media are considered to be much smaller than the considered wavelength, so as to neglect the quantum-size effect (or the subband structure). The respective contributions of media 1 and 2 to the inverse Green's function at the interface space of the composite system are given by Eq. (18). The inverse Green's function of the composite system is then obtained as an infinite banded matrix $g_\infty^{-1}(MM)$ defined in the interface domain constituted of all the sites n.

To find the contribution of medium 1 to the diagonal elements of the matrix $g_\infty^{-1}(MM)$ one has to take the element $g_1^{-1}(0,0)[=g_1^{-1}(d_i,d_i)]$ of Eq. (18) and multiply it by 2 (because at each site we have two pasted segments belonging to medium 1). The contribution of medium 2 to the diagonal elements is obtained by calculating the inverse of the matrix given by Eq. (18), taking the element $g_2(0,0)$ $[=g_2(d_i,d_i)]$, finding its reciprocal and multiplying it by N'. Therefore, the diagonal elements of the matrix

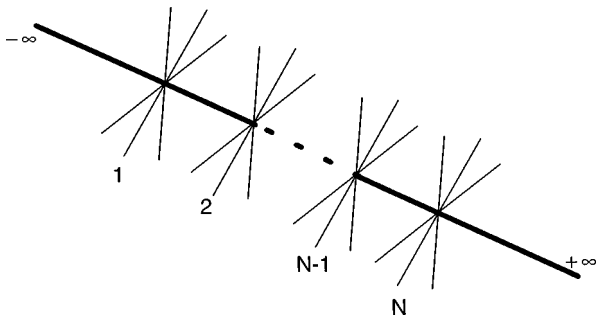

FIG. 2. Waveguide with $N'=6$ DSB of length d_2 grafted at a *finite number N* of equidistant sites separated by a length d_1 and connected at its extremities to two semi-infinite leading lines.

$g_\infty^{-1}(MM)$ are given by $-\{2(F_1C_1/S_1)+N'(F_2S_2/C_2)\}$. The off-diagonal elements are given by F_1/S_1 [see Eq. (18)].

Taking advantage of the translational periodicity of the system in the direction x_3, this matrix can be Fourier transformed as

$$[g_\infty(\mathbf{k},MM)]^{-1}=\frac{2F_1}{S_1}[-\xi+\cos(kd_1)], \tag{20}$$

where k is the modulus of the one-dimensional reciprocal vector $\mathbf{k}$, d_1 stands for the period of the system and $\xi=C_1+(N'F_2/2F_1)(S_1S_2/C_2)$.

The dispersion relation of the infinite periodic comblike waveguide is given by Eq. (5), that is, $[g_\infty(k,MM)]^{-1}=0$. This relation takes the simple form

$$\cos(kd_1)=C_1+\frac{N'F_2}{2F_1}\frac{S_1S_2}{C_2}. \tag{21}$$

On the other hand, in the $\mathbf{k}$ space, the Green's function of the infinite homogenous magnonic waveguide is

$$g_\infty(\mathbf{k},MM)=\frac{S_1}{F_1}\frac{1}{\{-2[\xi-\cos(kd_1)]\}}. \tag{22}$$

After inverse Fourier transformation, Eq. (22) yields[38]

$$g_\infty(n,n')=\frac{S_1}{F_1}\cdot\frac{t^{|n-n'|+1}}{t^2-1}, \tag{23}$$

where the integers n and n' refer to the sites $(-\infty<n,n'<+\infty)$ on the infinite line and the parameter t is given by

$$t=e^{jkd_1}. \tag{24}$$

B. Transmission coefficient of the finite comblike structures

Infinite magnonic comblike structures are not physically realizable but finite comb structures are. Therefore, in this section, we investigate the transmission properties of a finite comb. This comb, as represented in Fig. 2, is constructed as follows: a finite piece containing N equidistant groups of DSB is cut out of the infinite periodic system illustrated in Fig. 1, and this piece is subsequently connected at its extremities to two semi-infinite leading lines. The finite comb is therefore composed of N' DSB (medium 2) of length d_2 grafted periodically with a spacing period d_1 at N sites on a finite line (medium 1), N and N' being integers. For the sake of simplicity, the semi-infinite leads and medium 1 are assumed to be constituted of the same material. We calculate analytically the transmission coefficient of a bulk spin wave coming from $x_3=-\infty$.

The system of Fig. 2 is constructed from the infinite comb of Fig. 1. In a first step, one suppresses the segments linking sites 0 and 1, and sites N and $N+1$. For this new system composed of a finite comb and two semi-infinite leads, the inverse Green's function at the interface space, $g_t^{-1}(MM)$, is an infinite banded matrix defined in the interface domain of all the sites n, $-\infty<n<+\infty$. This matrix is similar to the one associated with the infinite comb. Only a few matrix elements differ, namely, those associated with the sites $n=0$, $n=1$, $n=N$, and $n=N+1$.

The cleavage operator $\mathbf{V}_{\rm cl}(MM)=\mathbf{g}_{\mathbf{t}}^{-1}(MM)-\mathbf{g}_\infty^{-1}(MM)$,[29] is the following 4×4 square matrix defined in the interface domain constituted of sites 0, 1, N, $N+1$

$$V_{\rm cl}(MM)=\begin{pmatrix} A & -B & 0 & 0\\ -B & A & 0 & 0\\ 0 & 0 & A & -B\\ 0 & 0 & -B & A\end{pmatrix}, \tag{25a}$$

where

$$A=\frac{F_1C_1}{S_1}\quad\text{and}\quad B=\frac{F_1}{S_1}. \tag{25b}$$

In a second step, two semi-infinite leads constituted of the same material as medium 1 are connected to the extremities $n=1$ and $n=N$ of the finite comb. With the help of the IRT, one deduces that the perturbing operator $\mathbf{V_p}(MM)$ allowing the construction of the system of Fig. 2 from the infinite comb is then defined as the 4×4 square matrix [see Eq. (17)]

$$V_p(MM)=\begin{pmatrix} A & -B & 0 & 0\\ -B & A-F_1 & 0 & 0\\ 0 & 0 & A-F_1 & -B\\ 0 & 0 & -B & A\end{pmatrix}. \tag{26}$$

Using Eqs. (23) and (26), one obtains the matrix operator $\Delta(MM)=\mathbf{I}(MM)+\mathbf{V_p}(MM)\mathbf{g}_\infty(MM)$ in the space M of sites $n,n'=0$, 1, N, $N+1$. For the calculation of the transmission coefficient, we need only the matrix elements $\Delta(1,1)$, $\Delta(1,N)$, $\Delta(N,1)$, and $\Delta(N,N)$, which can be set in the form of a 2×2 matrix $\Delta_S(MM)$

$$\Delta_S(MM)=\begin{pmatrix} 1+Ct & Ct^N\\ Ct^N & 1+Ct\end{pmatrix} \tag{27a}$$

with

$$C=-\frac{[t-(C_1-S_1)]}{(t^2-1)}. \tag{27b}$$

The surface Green's function $d_s(MM)$ of the finite comb with two connected semi-infinite leads in the space of sites 1 and N is

$$d_S(MM)=g_S(MM)\Delta_S^{-1}(MM)=\frac{S_1}{F_1}\frac{t}{t^2-1}\frac{1}{\det\Delta_S(MM)}\times\begin{bmatrix}1+Ct(1-t^{2N-2}) & t^{N-1}\\ t^{N-1} & 1+Ct(1-t^{2N-2})\end{bmatrix}, \tag{28}$$

with

$$g_S(MM)=\frac{S_1}{F_1}\frac{t}{t^2-1}\begin{pmatrix}1 & t^{N-1}\\ t^{N-1} & 1\end{pmatrix} \tag{29}$$

and

$$\det\Delta_S(MM)=1+2Ct+C^2t^2(1-t^{2N-2}). \tag{30}$$

In Eq. (29), $g_S(MM)$ is the matrix constituted of elements of $g_\infty(MM)$ associated with sites 1 and N. We now calculate the transmission coefficient with a bulk spin wave coming from, $x_3=-\infty$, $U(x_3)=e^{-\alpha_1 x_3}$. Substituting this incident wave in Eq. (6) and considering Eqs. (15) and (28), we obtain the transmitted wave $u(x_3')$, with $x_3'\geqslant Nd_1$, as

$$u(x_3')=-2S_1\cdot\frac{t^N}{t^2-1}\cdot\frac{e^{-\alpha_1[x_3'-(N-1)d_1]}}{\det\Delta_S(MM)}. \tag{31}$$

One deduces that the transmission coefficient is

$$T=\left|\frac{2S_1(t^2-1)}{t^{-N}[1-t(C_1-S_1)]^2-t^N[t-(C_1-S_1)]^2}\right|^2. \tag{32}$$

IV. LARGE MAGNONIC STOP BANDS AND TRANSMISSION SPECTRA

In this section, we analyze the band structure and the transmission factor of the one-dimensional comblike structure, namely Eqs. (21) and (32). One can notice from Eq. (21) that the pass bands are obtained when the right-hand side takes on values in the range $[-1, +1]$. In the limit $N'=0$, one simply recovers free-wave propagation along the backbone ($k\equiv\alpha_1'$, $T=1$). On the other hand, increasing the number N' will prevent the right-hand side of Eq. (21) from becoming smaller than unity and hence, contributes to decreasing the widths of the pass bands (or increasing the widths of the band gaps). However, at frequencies satisfying the conditions: $S_1=0$ or $S_2=0$, the right-hand side of Eq. (21) becomes one, and these frequencies necessarily fail inside the pass bands.

Equation (32) for the transmission factor T in the case $N=1$ can be written as

$$T=\left|\frac{2F_1C_2}{N'F_2S_2+2F_1C_2}\right|^2. \tag{33}$$

It is clear that this coefficient equals zero when $C_2=0$, i.e.,

$$\alpha_2'd_2=(m+\tfrac{1}{2})\pi. \tag{34}$$

The corresponding frequency will be

$$\omega_g=\gamma_2H_0+D_2'\left\{(m+\tfrac{1}{2})\frac{\pi}{d_2}\right\}^2 \tag{35a}$$

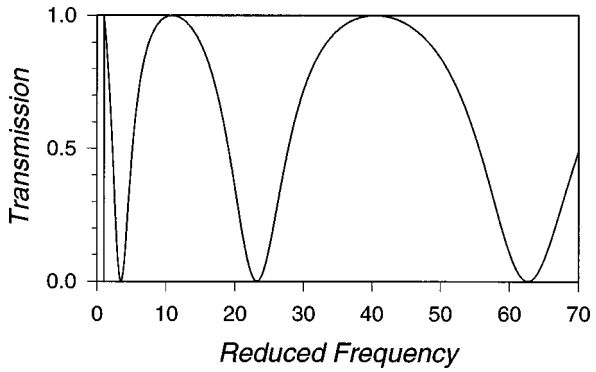

FIG. 3. Transmission coefficient versus reduced frequency for a waveguide with $N=N'=1$ in the case of identical media 1 and 2. For convenience H_g is considered to be 1.

or symbolically

$$\Omega_g=H_g+\{(m+\tfrac{1}{2})\pi\}^2, \tag{35b}$$

where m is a positive integer, $\Omega_g=\omega_g d_2^2/D_2'$ is a reduced frequency, and $H_g=\gamma_2H_0d_2^2/D_2'$. From the above equation one can notice that for this composite system there exists an infinite set of forbidden frequencies Ω_g corresponding to the eigenmodes of the DSB. These DSB work as resonators and, consequently, this composite system filters out the frequencies Ω_g. One also observes from Eq. (34) that T is equal to zero when $\alpha_2'd_2$ is an odd multiple of $\pi/2$. T reaches its maximum value of 1 when $\alpha_2'd_2$ is a multiple of π. This latter case is illustrated in Fig. 3. In the case $N>1$, the zeros of the transmission coefficient enlarge into gaps. It is worth mentioning that the existence of transmission zeros has already been demonstrated in wave guides with a resonantly coupled stub for electrons,[28] phonons,[39–40] photons,[41] and acoustic waves.[42] This phenomenon is related to the resonances associated with the finite additional path offered to the wave propagation.

We now turn to discussing our numerical results for the band structure and transmission coefficient. We limit ourselves to the case of *identical media* ($\alpha_1'=\alpha_2'$) constituting the backbone and the side branches. Finally, we also consider simple combs with $N'=1$ and for which the length of the distance between DSB amounts to the length of the side branches (i.e., $d_1=d_2$). Equation (21) then reduces to a second-order polynomial equation that can be straightforwardly solved for the frequency to give

$$\Omega=\tilde{H}+\{\arccos[(1/3)(\cos(kd_1)\pm\sqrt{\cos^2(kd_1)+3})]\}^2, \tag{36}$$

where $\Omega=\omega d_1^2/D_1'$ is the reduced frequency and $\tilde{H}=\gamma_1H_0d_1^2/D_1'$. The plus and minus signs give the two solutions of the second-order polynomial equation. The arccos function appearing on the right-hand side of Eq. (36) shows that there are an infinite number of dispersion curves that are repeated periodically. In Fig. 4(a) we only show the first seven dispersion curves in the band structure of the infinite comb composite. There is a complete absolute gap below the lowest band due to the presence of the external field H_0. There exist other absolute gaps, between the first and the second bands, the second and the third bands, the fourth and

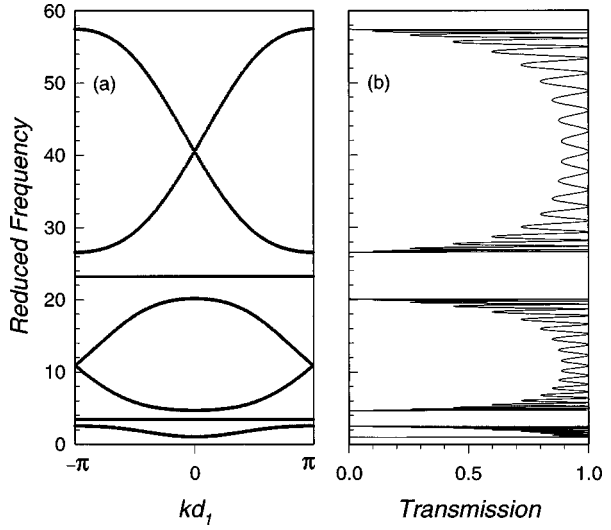

FIG. 4. (a) The first seven bands, in the magnonic band structure of the infinite periodic comb. We have chosen $d_1=d_2$, $D_1'=D_2'$, $\tilde{H}=1$, $N'=1$, and $N\to\infty$. The plot is given as the reduced frequency versus the dimensionless quantity kd_1 ($-\pi\leqslant kd_1\leqslant+\pi$), where k is the modulus of the propagation vector. One observes an absolute gap below the first band due to the presence of the external field H_0. (b) Transmission coefficient versus the reduced frequency for a waveguide with $N'=1$ and $N=10$. The other parameters are the same as in Fig. 4(a).

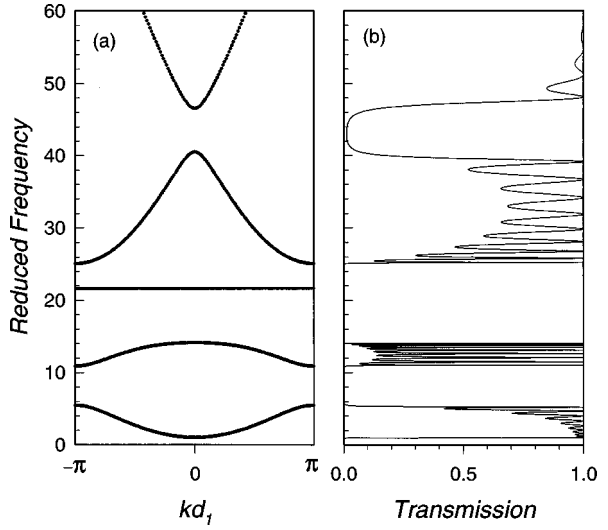

FIG. 5. (a) The first five bands in the band structure of the infinite periodic comb with $d_2=0.4d_1$, $N'=1$, and $N\to\infty$. The two media are identical. (b) The transmission factor T for $N=10$, $N'=1$, and $\tilde{H}=1$. The other parameters are the same as in Fig. 5(a).

the fifth bands, and between the fifth and the sixth bands. The second and the fifth bands are flat bands, which correspond to localized modes inside each resonator. *These modes do not penetrate into the backbone*. The tangential points between the third and the fourth bands are degenerate points, they appear at $kd_1=\pi$ and $-\pi$. Another degenerate point is the tangential point between the sixth and the seventh bands that appears at $kd_1=0$. One can also notice antisymmetry between the third and fourth bands and between the sixth and seventh bands as well. This antisymmetry is clearly visible when plotting the corresponding transmission factor. Figure 4(b) shows the frequency dependence of the transmission for $d_2=d_1$, $N'=1$ and $N=10$. The flat bands in Fig. 4(a), associated with localized modes inside the resonators (i.e., $C_2=0$), do not contribute to the transmission. The number of oscillations in the transmission factor within the pass bands, which corresponds to the third and the fourth or to the sixth and seventh bands, has been noted to be unfailingly $2N-1$. This number is $N-1$ within the pass band, which corresponds to the band that has no tangential points with any other bands (see also Fig. 5).

Figure 5(a) shows the first five bands for the case of two identical media with $d_2=0.4d_1$ and $N'=1$. The third band is flat. As previously noted, such a band corresponds to localized modes inside the resonators. One can notice that a decrease or an increase in the length of the DSB removes the degenerate points. The transmission factor is also influenced by this change in geometry. This phenomenon is illustrated in Fig. 5(b) [N and N' have the same values as in Fig. 4(b)]. Interestingly the width of the pass bands (stop bands) decreases (increases) with this other choice of the length d_2. A comparison between Figs. 4(b) and 5(b) indicates that the number of sites in the comb N is important in achieving completely formed gaps. This number is of the order of $N\approx 6$ in Fig. 4(b) where $d_2=d_1$ (similar results are obtained for $d_2/d_1=0.5, 1, 1.5, 2, 2.5, \ldots$), while it becomes of the order of $N>10$ in Fig. 5(b) with $d_2=0.4d_1$.

Figure 6 depicts the effect of variation in the number N of sites on the transmission factor T for a finite comb constituted of two identical media with $d_1=d_2$. We show the frequency dependence of the transmission for $N'=1$ and $N=2$, 5, and 10 in the top, middle, and bottom panels, respec-

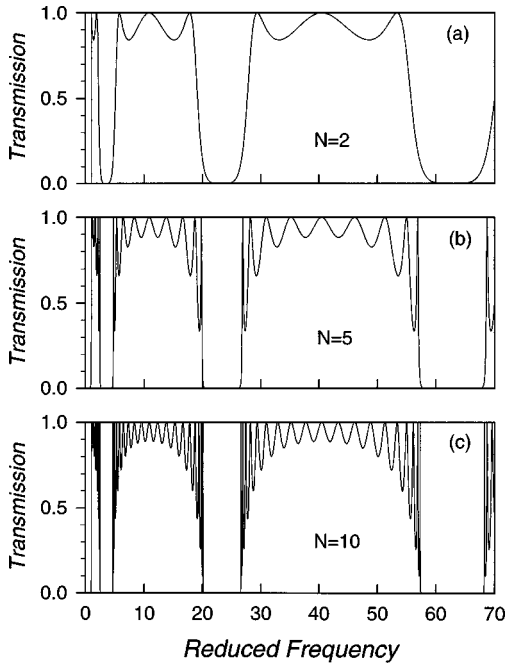

FIG. 6. Transmission coefficient versus the reduced frequency for several values of $N(N'=1)$. Both media are considered to be identical, $\tilde{H}=1$, and $d_1=d_2$. The top, middle, and bottom panels depict the transmission for $N=2$, 5, and 10, respectively. Note that increasing N results in turning some of the pseudogaps into complete gaps, but leaves their widths virtually intact.

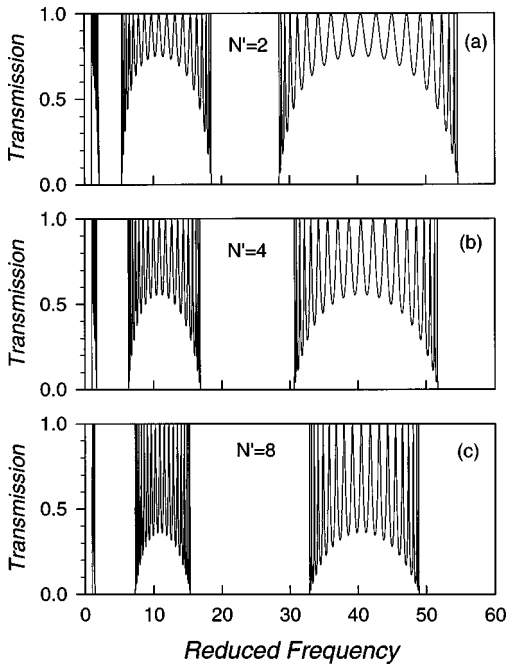

FIG. 7. Same as in Fig. 6, except that now N' is varied ($N=10$ is fixed). The top, middle, and bottom panels depict the transmission for $N'=2$, 4, and 8, respectively. Noteworthy is the shrinking (widening) of the pass-bands (stop bands) with increasing N'. We call attention to the increasing of the oscillation amplitudes with increasing N'.

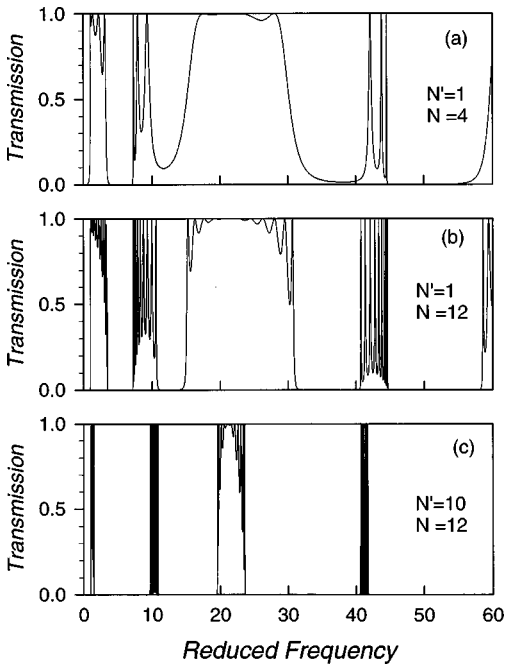

FIG. 8. Transmission coefficient versus the reduced frequency for the waveguide with $d_2=0.7d_1$. The two media are identical and $\tilde{H}=1$. In the top and middle panels $N'=1$ and N equals 4 and 12 while in the middle and bottom panels $N=12$ and N' equals 1 and 10. It is noticeable that the width of the pass bands (stop bands) decreases (increases) with increasing N'.

tively. It is apparent again that as N increases the pseudogaps in the transmission turn into full gaps. However, one does not need exceedingly large values of N, at the reasonably small value of $N=5$ the gaps are already formed. Moreover, for a given frequency range, there is an optimum value of N above which any additional increment in N leaves the bands practically unaffected.

Next, we discuss the dependence of the transmission factor on the number of dangling side branches. The results are illustrated in Fig. 7 for three values of N' in the case of two identical media with $d_1=d_2$. The top, middle and bottom panels display the frequency dependence of the transmission for $N=10$ and $N'=2$, 4, and 8, respectively. We call attention to the fact that the width of the pass bands (stop bands) decreases (increases) with increasing number of DSB. We can also note that an increase in N' results in an increase in the amplitude of oscillations of the transmission coefficient.

Let us stress that, unlike in the usual two-dimensional composite system where the contrast in physical properties between the constituent materials is a critical parameter in determining the existence of the gaps,[8] the occurrence of narrow magnonic bands, *does not require the use of two different materials*. In other words, the magnonic structure is tailored within a single homogenous medium, although the boundary conditions impose the restriction that the waves only propagate in the interior of the waveguides.

Finally, we end this section with an investigation of the influence of the geometry on the transmission of the comb-like systems. We compute the frequency dependence of the transmission factor for $d_2=0.7d_1$. The results are displayed in Fig. 8, in the top and middle panels with N' $(=1)$ kept fixed and N taking the values 4 and 12, respectively. One can notice that varying N results in turning the pseudogaps into full gaps. The convergence to full gaps can be achieved in general for a reasonably small number of sites. In the middle and bottom panels N $(=12)$ is kept fixed and N' takes the values 1 and 10, respectively. The most interesting feature is that the width of the pass bands (stop bands) decreases (increases) with increasing N'. On comparing the results of Figs. 8 and 7, one can notice the same qualitative behavior, but with a more significant widening of the gaps in Fig. 8 with increasing N'.

As is clear from Eq. (21), the pass bands described in the above applications are mainly concentrated around frequencies satisfying either $S_1=0$ or $S_2=0$. These conditions involve the two characteristic lengths d_1 and d_2, which means that the bands originate either from the periodicity of the system or from the resonance states of each DSB. On the other hand, the narrowness of the bands suggests that the condition for constructive interference can only be satisfied in small frequency intervals, in relation with the numbers N and N'. If one first considers the scattering of an incoming wave by the DSB at a single site (i.e. $N=1$), Eq. (32) easily reveals that the transmission will be suppressed if one increases the number N' of DSB [see Eq. (33)], except at frequencies where $S_2\approx 0$. Now, grafting the DSB's at two or more sites on the backbone (i.e., $N\geqslant 2$) opens new channels for transmission at frequencies in the vicinity of the frequency corresponding to the solutions of $S_1=0$. This means that the condition for constructive interference is allowed in small intervals whose frequencies are related to the new characteristic length d_1. These pass bands slightly increase in width upon increasing the number N of sites. At the same time, for a given N, increasing N' gives rise to tighter con-

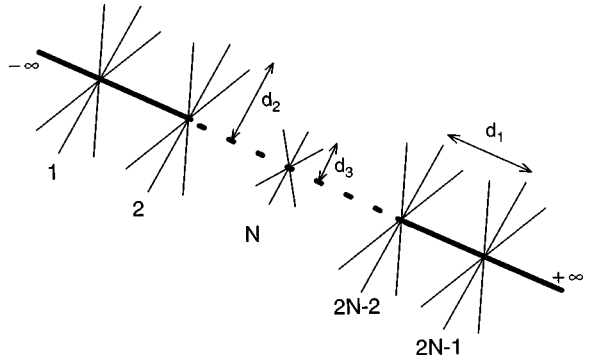

FIG. 9. Same as in Fig. 2 except that a defect composed of $N_3'=6$ DSB of length d_3 is introduced in the middle of the finite comb and $N'=6$. For simplicity the total number of sites is considered to be odd.

dition for constructive interference, thus contributing to a reduction in width of the pass bands.

V. DEFECT MODES

In this section, we investigate the existence of localized modes inside the gaps when defect dangling side branches of length d_3 are inserted at one site of the waveguide (see Fig. 9). With the help of the interface response theory[29] one can arrive, analytically, at the following result for the localized states in the case of an infinite comb ($N\rightarrow\infty$),

$$1+\frac{S_1}{F_1}\left(N'\frac{F_2S_2}{C_2}-N_3'\frac{F_3S_3}{C_3}\right)\frac{t}{t^2-1}=0. \tag{37}$$

In the preceding relation, N_3' stands for the number of the defect DSB and the rest of the symbols have their usual meaning.

Next, with the help of Eq. (37) we study the effects of variation in the length of the defect branch on the existence of localized states. We assume that our system is composed of identical media and that $N'=N_3'=1$ and $d_2=d_1$. Figure 10 gives the frequencies of the localized modes as functions of the ratio d_3/d_1. The hatched areas correspond to the bulk bands of the perfect comb. The frequencies of the localized modes are very sensitive to the length d_3. The localized modes emerge from the bulk bands, decrease in frequency with increasing length d_3, and finally merge into a lower bulk band where they become resonant states. At the same time, new localized modes emerge from the bulk bands. Let us note that for any given reduced frequency in Fig. 10, there is a periodic repetition of the modes as functions of d_3/d_1.

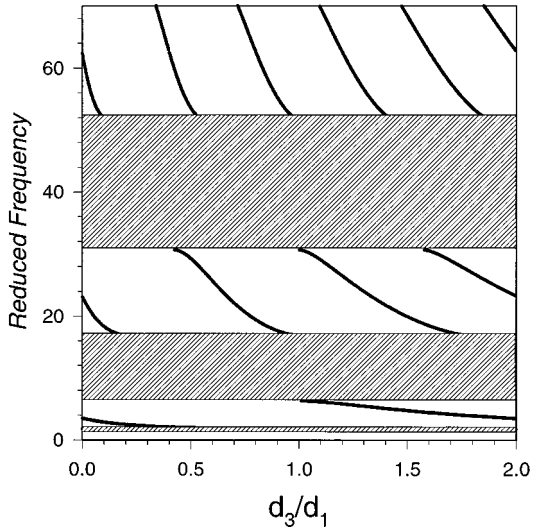

FIG. 10. Frequencies of the localized modes associated with N_3' defect DSB of length d_3 in an infinite comb. The other parameters are $N'=N_3'=4$, $N\rightarrow\infty$, $d_2=d_1$, and $\tilde{H}=1$. The system is assumed to be composed of identical media.

Under the assumption that the defects are located in the middle of a finite comb (for simplicity one can take the number of sites to be odd see Fig. 9), we have obtained an analytical expression for the transmission factor T through the defective comb

$$T=\left|\frac{2F_1B_2^2}{(B_1-F_1)[(B_1-F_1)(B_3+2B_1+2N'F_2S_2/C_2)-2B_2^2]}\right|^2, \tag{38}$$

where

$$B_1=\frac{F_1}{S_1}\frac{[C_1(t-t^{2N-1})+t^{2N}-1]}{t(1-t^{2(N-1)})}, \tag{39}$$

$$B_2=\frac{F_1}{S_1}\frac{(t^{N-1}-t^{N+1})}{t(1-t^{2(N-1)})}, \tag{40}$$

and

$$B_3=-N_3'\frac{F_3S_3}{C_3}. \tag{41}$$

The transmission coefficient is also affected by the presence of a defect inside the comb. In particular, T exhibits narrow peaks associated with the localized modes. In Fig. 11, we compare the transmission coefficients for two combs with and without defects. The results are illustrated for $N'=N_3'=4$, $N=5$, $d_2=d_1$, and $d_3=1.3d_1$. Figure 11(b) shows one localized mode in the second, the third, and the fourth gaps. The localized mode inside the third forbidden band lies in the middle of the gap while the localized modes in the other

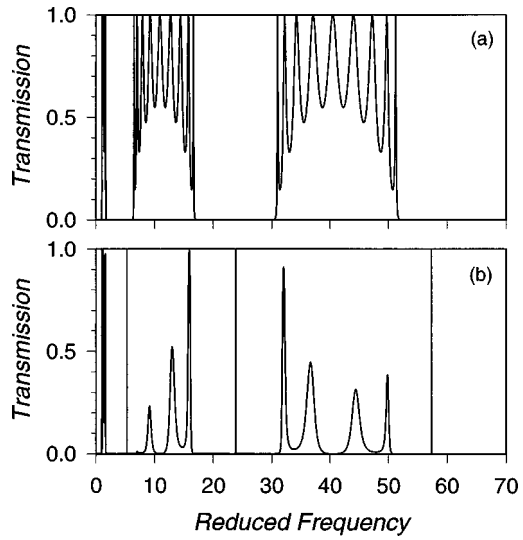

FIG. 11. Transmission coefficients versus the reduced frequency for two combs with (b) and without (a) defect. The results are illustrated for $N'=N_3'=4$, $N=5$, $d_2=d_1$, $d_3=1.3d_1$, and $\tilde{H}=1$. In the frequency range displayed in this figure one can see that the peaks falling in the gap are very narrow. Transmission inside a bulk band is significantly affected by the presence of a defect.

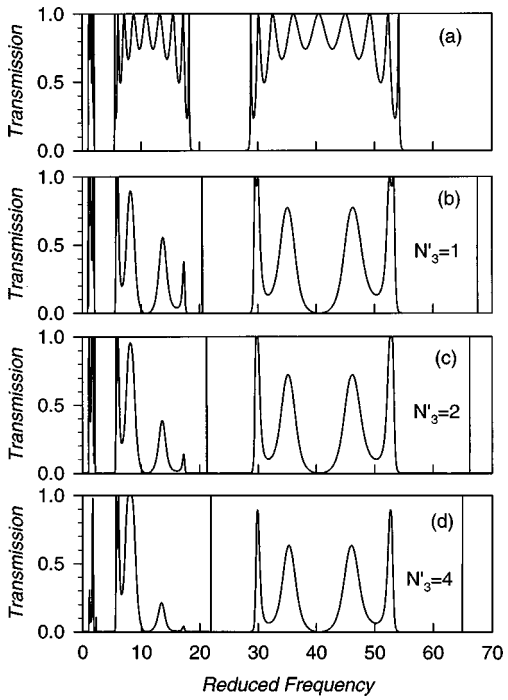

FIG. 12. Transmission coefficients, T, versus the reduced frequency for four combs with [(b), (c), (d)] and without (a) defect. In the panels (b), (c), and (d), N_3' equals 1, 2, and 4 respectively. The results are illustrated for $N'=2$, $N=5$, $d_2=d_1$, $d_3=0.75d_1$, and $\tilde{H}=1$. With increasing N_3', T is depressed in the bands and the localized mode is approaching the center of the gap.

two gaps lie closer to the bulk bands. As one can see, the second bulk band is asymmetric due to the proximity of the first localized mode to its left side. The situation is similar for the third pass band, but the asymmetry is due to the proximity of the localized mode to its right. In the frequency range displayed in this figure one can see that the peaks corresponding to the localized modes are very narrow. The transmission inside a bulk band can also be significantly affected by the presence of a defect. For instance, in the example shown in Fig. 11, T is significantly depressed in the second and third bulk bands.

Finally, we end this section with a study of the influence of N_3' on the transmission factor. Figure 12 shows a comparison of the transmission coefficients for four combs with N_3' varying from zero (top panel) to 1, 2, and 4. The results are illustrated for $N'=2$, $N=5$, $d_2=d_1$, and $d_3=0.75d_1$. One notices that the transmission factor in the bands is depressed as N_3' increases. Figures 12(b), 12(c), and 12(d) show one localized mode in the third and fourth gaps. One can also observe from Fig. 12 that the localized mode is getting closer to the middle of the gap when N_3' increases. One notes also from Fig. 12(b) to Fig. 12(d), that the localized modes become more and more confined, i.e., the quality factor of the corresponding peaks increases, with increasing N_3'.

VI. CONCLUSIONS

The purpose of this work was to investigate theoretically the magnonic band structure of one-dimensional comb structures composed of multiple dangling side branches N' grafted at N equidistant sites along a backbone. There exist large absolute band gaps in the magnonic band structure of an infinite periodic comb with MDSB. The calculated transmission spectrum of spin waves in finite comb structures parallels the band structure of the infinite periodic combs. The existence of the gaps in the spectrum is attributed to the joint effect of pseudoperiodicity and the resonance states of the grafted dangling side branches. In these systems, the gap width is controlled by the numbers N and N', the geometrical parameters, including the length of the side branches and the periodicity of the comb, as well as the contrast in the physical properties of side branches material and the backbone. Nevertheless, the magnonic band structure exhibits relatively wide gaps for chemically homogeneous systems where the branches and the substrate are constituted of the same material. We have also shown that devices composed of finite numbers of sites exhibit a behavior similar to that of an infinite periodic comb.

Localized states associated with defects in the comb were observed. These defect modes appear as narrow peaks of strong amplitude in the transmission spectrum. Since magnetic periodic composites have, in general, wide technical applications, it is anticipated that this new class of materials, which can be referred to as ''magnonic crystals'', may turn out to be of significant value for prospective applications. Especially, one would expect such applications to be feasible in electronics (spin-wave electronics), since magnon excitation energies also fall in the microwave range. Of special interest is the prospect of achieving a complete band gap; this defined to be a stop band in which magnons are prohibited for all values of the wave vector.

At this stage it is worth pointing out again the conditions of validity of the model. In all our calculations we have assumed that the cross section of the waveguide is small compared to its linear dimension, that is, the waveguide may

be considered as a one-dimensional medium. However it would be interesting to verify the extension of the band gaps in the two-dimensional Brillouin zone of thicker wires. The calculation of the band structure in this case will be the subject of future work as well as the study of magnonic properties of more complex structures.

ACKNOWLEDGMENT

One of us (H.A.) would like acknowledge the hospitality of the ''Laboratoire de Dynamique et Structures des Matériaux Moléculaires,'' U.F.R. de Physique, Université de Lille I, where this work was done.

*Permanent address: Faculty of Engineering, Zagazig University, Benha Branch, Cairo, Egypt.

†Author to whom correspondence should be addressed. Electronic address: akjouj@lip5rx.univ-lille1.fr

[1] M. Greven, R. J. Birgeneau, and U.-J. Wiese, Phys. Rev. Lett. **77**, 1865 (1996).

[2] S. Chakravarty, Phys. Rev. Lett. **77**, 4446 (1996).

[3] D. G. Shelton, A. A. Nersesyan, and A. M. Tsvelik, Phys. Rev. B **53**, 8521 (1996); J. Piekarewicz and J. R. Shepard, *ibid.* **57**, 10 260 (1998).

[4] E. L. Albuquerque, P. Falco, E. F. Sarmento, and D. R. Tilley, Solid State Commun. **58**, 41 (1986).

[5] L. Dobrzynski, B. Djafari-Rouhani, and H. Puszkarski, Phys. Rev. B **33**, 3251 (1986).

[6] J. Barnas, Phys. Rev. B **45**, 10 427 (1992).

[7] L. L. Hinchey and D. J. Mills, Phys. Rev. B **33**, 3359 (1986); **34**, 1689 (1986).

[8] J. O. Vasseur, L. Dobrzynski, B. Djafari-Rouhani, and H. Puszkarski, Phys. Rev. B **54**, 1043 (1996).

[9] M. S. Kushwaha, P. Halevi, L. Dobrzynski, and B. Djafari-Rouhani, Phys. Rev. Lett. **71**, 2022 (1993).

[10] M. S. Kushwaha and P. Halevi, Appl. Phys. Lett. **69**, 31 (1996); M. S. Kushwaha and B. Djafari-Rouhani, J. Appl. Phys. **81**, 3191 (1996).

[11] L. Dobrzynski, B. Djafari-Rouhani, J. O. Vasseur, R. Kucharczyk, and M. Steslicka, Prog. Surf. Sci. **48**, 213 (1995).

[12] E. Yablonovitch, Phys. Rev. Lett. **58**, 2059 (1987).

[13] S. John, Phys. Rev. Lett. **58**, 2486 (1987).

[14] S. John, Phys. Rev. Lett. **53**, 2169 (1984).

[15] M. S. Kushwaha, Int. J. Mod. Phys. B **10**, 977 (1996).

[16] See for example, J. D. Joannopoulos, R. D. Meade and J. N. Winn, *Photonic Crystals* (Princeton University Press, Princeton, 1995); in *Photonic Band Gap Materials*, edited by C. M. Soukoulis (Kluwer, Dordrecht, 1996).

[17] M. Sigalas, C. M. Soukoulis, E. N. Economou, C. T. Chan, and K. M. Ho, Phys. Rev. B **48**, 14 121 (1993).

[18] E. Yablonovitch, T. J. Gmitter, R. D. Meade, A. M. Rappe, K. D. Brommer, and J. D. Joannopoulos, Phys. Rev. Lett. **67**, 3380 (1991).

[19] A. Mekis, J. C. Chen, I. Kurland, S. Fan, P. R. Villeneuve, and J. D. Joannopoulos, Phys. Rev. Lett. **77**, 3787 (1996).

[20] K. Sakoda and H. Shiroma, Phys. Rev. B **56**, 4830 (1997).

[21] S. Foresi, P. R. Villeneuve, J. Ferrera, E. R. Thoen, G. Steinmeyer, S. Fan, J. D. Joannopoulos, L. C. Kimerling, Henry I. Smith, and E. P. Ippen, Nature (London) **390**, 143 (1997).

[22] M. Uehara *et al.*, J. Phys. Soc. Jpn. **65**, 2764 (1996).

[23] A. Blondel, J. P. Meier, B. Boudin, and J. P. Ansermet, Appl. Phys. Lett. **65**, 3019 (1994).

[24] J. de la Figuera, M. A. Huerta-Garnica, J. E. Prioto, C. Ocal, and R. Miranda, Appl. Phys. Lett. **66**, 1006 (1995).

[25] W. Z. Li, S. S. Xie, L. X. Qian, B. H. Chang, B. S. Zou, W. Y. Zhou, R. A. Zhao, and J. Wang, Science **274**, 1701 (1996).

[26] See, e.g., *The Handbook of Microlithography, Micromachining, and Microfabrication,* edited by P. Rai-Chaudhry (SPIE, Bellingham, MA, 1996).

[27] Jian-Bai Xia, Phys. Rev. B **45**, 3593 (1992).

[28] W. Porod, Z. Shao, and C. S. Lent, Appl. Phys. Lett. **61**, 1350 (1992).

[29] L. Dobrzynski, Surf. Sci. Rep. **11**, 139 (1990).

[30] F. Sols, M. Maccuci, U. Ravaioli, and K. Hess, J. Appl. Phys. **66**, 3892 (1989).

[31] P. Singha Deo and A. M. Jayannavar, Phys. Rev. B **50**, 11 629 (1994).

[32] M. E. Gershenson, P. M. Echternach, A. G. Mikhalchuk, and H. M. Bozler, Phys. Rev. B **51**, 10 256 (1995).

[33] L. Dobrzynski, J. Mendialdua, A. Rodriguez, S. Bolibo, and M. More, J. Phys. (France) **50**, 2563 (1989).

[34] T. G. Phillips and H. M. Rosenberg, Rep. Prog. Phys. **29**, 285 (1966).

[35] M. G. Cottam and A. A. Maradudin, in *Surface Excitations,* Modern Problems in Condensed Matter Sciences Vol. 9 (North-Holland, Amsterdam, 1984).

[36] A. Akjouj, B. Sylla, and L. Dobrzynski, Ann. Phys. (Paris) **18**, 363 (1993).

[37] M. L. Bah, Ph.D. thesis, University of Lille I, 1995.

[38] E. N. Economou, *Green's Functions in Quantum Physics* (Springer-Verlag, Berlin, 1983), p. 79.

[39] L. Dobrzynski, B. Djafari-Rouhani, P. Zielinski, A. Akjouj, B. Sylla, and E. Oumghar, Acta Phys. Pol. A **89**, 139 (1996).

[40] P. A. Deymier, E. Oumghar, J. O. Vasseur, B. Djafari-Rouhani, and L. Dobrzynski, Prog. Surf. Sci. **53**, 179 (1997).

[41] J. O. Vasseur, P. A. Deymier, B. Djafari-Rouhani, L. Dobrzynski, and A. Akjouj, Phys. Rev. B **55**, 10 434 (1997); L. Dobrzynski, A. Akjouj, B. Djafari-Rouhani, J. O. Vasseur, and J. Zemmouri, *ibid.* **57**, R9388 (1998).

[42] M. S. Kushwaha, A. Akjouj, B. Djafari-Rouhani, L. Dobrzynski, and J. O. Vasseur, Solid State Commun. **106**, 659 (1998).